Journal of the European Ceramic Society **11** (1993) 171–177

TEM Characterization of Nickel and Nickel–Cobalt Manganite Ceramics

M. Brieu,[a] J. J. Couderc,[b] A. Rousset[a] & R. Legros[a]

[a] Laboratoire de Chimie des Matériaux Inorganiques, CNRS URA 1311—Université Paul Sabatier, 118, route de Narbonne—31062-Toulouse-Cédex, France
[b] Laboratoire de Physique des Solides, CNRS URA 74—Université Paul Sabatier et Institut National de Sciences Appliquées, Complexe Scientifique de Rangueil, 31077-Toulouse-Cédex, France

(Received 20 January 1992; revised version received 2 April 1992; accepted 13 April 1992)

Abstract

Nickel and nickel–cobalt manganites were investigated by transmission electron microscopy (TEM) in order to relate microstructure and phase composition to the electrical stability of these ceramics after ageing. The air-quenched samples are biphased and exhibited a perturbed microstructure with bidimensional lattice defects. It is shown that the improvement in the stability of electrical properties is not due to the existence of a precipitated phase, like NiO, but could be related to the presence of a 'tweed' structure, that is, a fine periodic structure built on {110} lamellae (exsolutions). Since the change in the electrical properties could be related to the Mn^{3+} cluster migration, it is suggested that the lattice perturbations resulting from the 'tweed' could slow down cluster migration and then stabilize the electrical properties of the ceramics studied.

Nickel- und Nickel–Kobalt-Manganitzusammensetzungen wurden mittels Transmissionselektronenmikroskopie (TEM) untersucht, um den Zusammenhang zwischen Gefüge und Phasenzusammensetzungen und der elektrischen Stabilität dieser Keramiken nach einer Auslagerung von 1000 h bei 125°C zu ermitteln. Abgeschreckte Proben sind zweiphasig und zeigen ein gestörtes Gefüge mit zahlreichen zweidimensionalen Gitterdefekten. Es wird gezeigt, daß die Verbesserung der Stabilität der elektrischen Eigenschaften nicht auf die Existenz einer Ausscheidungsphase, wie beispielsweise NiO, zurückgeht, sondern mit der Präsenz einer 'Tweed'-artigen Struktur zusammenhängt, die aus periodisch angeordneten Lamellen längs {110} besteht. Da die Veränderung der elektrischen Eigenschaften auf die Wanderung von Mn^{3+}-Clustern zurückgeführt wird, wurde angenommen, daß die Gitterdefekte, die die beschriebene 'Tweed'-Struktur zur Folge haben, die Wanderung der Cluster verlangsamen und damit die elektrischen Eigenschaften der untersuchten Keramiken stabilisieren.

On étudie par microscopie électronique en transmission (MET) des manganites de nickel et de nickel–cobalt afin de relier leur microstructure et leur composition à leur stabilité électrique après un vieillissement de 1000 h à 125°C. Les échantillons trempés à l'air sont biphasés et révèlent une microstructure très perturbée avec de nombreux défauts plans. On montre que l'amélioration de la stabilité électrique n'est pas liée à l'existence d'une phase précipitée intergranulaire telle que NiO, mais pourrait être due à la présence d'une structure en 'tweed' (structure modulée formée de fines lamelles {110}). Puisque les variations des propriétés électriques semblent liées à la formation de clusters Mn^{3+}, on peut supposer que les perturbations du réseau qu'entraîne la structure en 'tweed' ralentissent cette migration et, par conséquent, stabilisent les propriétés électriques des céramiques étudiées.

1 Introduction

Transition-metal manganites $Mn_{3-x}M_xO_4$ ($O \leq x \leq 1$) and M = nickel, copper, cobalt, etc. form a group of semiconductors; the electrical transport phenomena of these materials are frequently interpreted in terms of phonon-assisted jumps of carriers among localized states, the so-called hopping conductivity.[1,2] The stability of these electrical properties under thermal constraint is a problem which can limit their practical use in applications as NTC thermistors. In previous papers it has been shown that stability can be greatly improved by quenching samples after sintering, and thus by the presence of precipitated phases at grain boundaries.[3–5] A correlation could be expected between

Journal of the European Ceramic Society 0955-2219/93/$6.00

the presence of precipitated phases and the stability of electrical properties. It can be assumed that insulating phases at the grain boundaries lead to a smooth transition from a grain-governed hopping mechanism to a grain boundaries-governed conduction mechanism, giving rise to a potential barrier set-up. However, in a recent communication[6] the authors reported that the so-called 'varistor effect' could not be detected. In a first approach, conduction is a result of the hopping mechanism, the precipitated phases not seeming to play any role in the conduction process.

Further experimental investigations involving studies of both charge carrier mobility and fine microstructure characterization of the ceramic grains are needed. This communication reports a transmission electron microscopy (TEM) study of nickel manganites and nickel–cobalt manganites both for single-phase and multiphase ceramics.

Many complex structures, including planar defects, were observed in some samples, particularly the quenched ones. In this paper, the authors intend only to give a first survey of the various phases encountered; a more detailed study is currently in progress.

2 Experimental Procedures

2.1 Preparation of ceramics

The low-temperature (600–700°C) decompositions of mixed oxalate precursors is a direct method for the preparation of homogeneous powders of manganite spinels allowing controlled morphology.[7] The oxide powders obtained were mixed with an organic binder pressed into disk form. The green disks were fired at 1200°C in air for 2 h. Two cooling treatments were carried out, slow cooling at 6°C/h, or air quenching; in this latter treatment, the samples were simply taken out of the furnace (mean cooling rate was 300°C/min). Metallographic observation showed that the ceramics are free from open porosity.

2.2 Measurement of electrical properties of ceramics

Samples for electrical measurements were prepared by depositing silver electrode on the opposite faces of the disk form. Electrical stability was measured by the variation of the resistance $\Delta R/R$ observed on ceramics after ageing (125°C for 1000 h in air).

2.3 Composition of samples

Two nickel manganites of formula $Mn_{2.25}Ni_{0.75}O_4$ and Mn_2NiO_4 and nickel–cobalt manganite $Mn_{1.85}Ni_{0.75}Co_{0.4}O_4$ were prepared. Two different batches were studied: slowly cooled at 6°C/h and quenched. The specifications of all the samples used in this study are listed in Table 1.

2.4 Preparation of samples for TEM

Samples for TEM observations were mechanically ground down to 50 μm, then thinned by ion milling. They were observed in a JEOL 200 CX electron microscope (TEMSCAN Service of the U.P.S., Toulouse) operating at 200 kV.

Thin-film X-ray spectroscopy was performed on the same electron microscope fitted with an energy-dispersive lithium-drifted silicon detector, a standard STEM attachment, and an EDAX 9100 spectrum analyser unit. This analytical method was used first in order to assist in an identification of the various phases present in each specimen. Semi-quantitative analysis with an accuracy of about 2% was also carried out.

3 TEM Observations

3.1 Nickel manganite

3.1.1 $Mn_{2.25}Ni_{0.75}O_4$

3.1.1.1 Slowly cooled. A single phase was detected: cubic spinel manganite ($a = 0{\cdot}843 \pm 0{\cdot}001$ nm) was perfectly identified by electron and X-ray diffraction. The grains (Fig. 1) of size around 15 μm are free from lattice defects such as dislocations or planar defects (stacking faults, twins, antiphase boundaries, etc.). Quantitative EDX analysis of the cations indicates fairly good homogeneity: Mn = 76·2–76·4 at.%, Ni = 23·6–23·8 at.%. Within the accuracy of the measurements, these values accord well with the theoretical chemical formula (Mn/Ni = 3).

3.1.1.2 Air quenched. The specimens are biphased: spinel manganite and nickel oxide (Fig. 2(a)). The

Table 1. Electric properties of the studied manganites

	Samples cooled at 6°C/h		*Samples air quenched*	
	ρ (Ω cm)[a]	$\Delta R/R$[b]	ρ (Ω cm)[a]	$\Delta R/R$[b]
Mn_2NiO_4	1 600	9	4 400	2
$Mn_{2.25}Ni_{0.75}O_4$	1 600	4	2 050	2·8
$Mn_{1.85}Ni_{0.75}Co_{0.4}O_4$	564	1·5	725	0·5

[a] ρ = Resistivity.
[b] $\Delta R/R$ = Relative value of the electric resistance after a 1000 h ageing at 125°C.

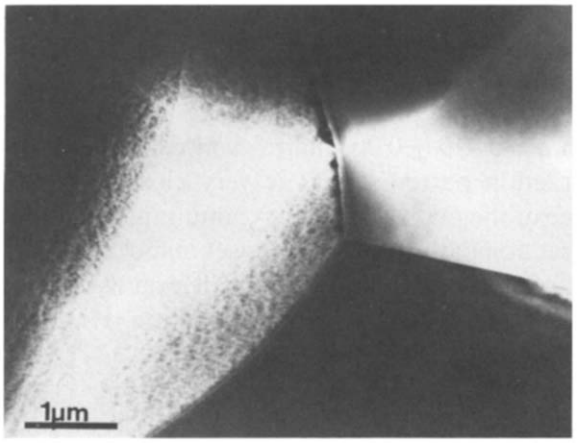

Fig. 1. Transmission electron micrograph (bright field) showing three grains of cubic spinel manganite in $Mn_{2\cdot25}Ni_{0\cdot75}O_4$ slowly cooled (monophased sample).

former phase has a mainly cubic structure with lattice parameter $a = 0{\cdot}852 \pm 0{\cdot}001$ nm as measured by X-ray diffraction; a splitting of the {311}–{113} line also indicates a slight tetragonalization of the cubic lattice of some grains. The size of the manganite grains (5–10 μm) is slightly decreased; the grains having a tetragonalized spinel structure contain a high density of thin lamellae (Fig. 2(b) and (c)) parallel to {110}. These lamellae are about 15–60 nm in width and generally fill up the whole grain; nevertheless, some heterogeneity is noted. Several groups of neighbouring grains are free from planar defects; it was observed that these grains, which do not exhibit a tetragonalization perceptible by electron diffraction, have a modulated structure ('tweed' structure) formed of very thin lamellae, a few nm in width and parallel to two sets of {110} planes quite similar to that observed on Fig. 9. Quantitative analysis of these grains shows a relative homogeneity: Mn = 78–80 at.%, Ni = 20–22 at.%. The Mn/Ni ratio is about 3·8; there is an impoverishment in Ni.

In the nickel oxide grains (≈ 1 μm), about 10 at.% of Mn was always detected by microanalysis (Fig. 2(a)). This result suggest that either Ni-substituted Mn or small manganite inclusions were present in the NiO grains, as observed in Mn_2NiO_4 (see Section 3.1.2).

Other grains presenting neither a 'tweed' structure nor a high density of lamellae are very heterogeneous, with Mn/Ni atomic ratio varying from 0·33 to 3·7. It can be concluded this is a closely mixed compound of NiO and spinel manganite.

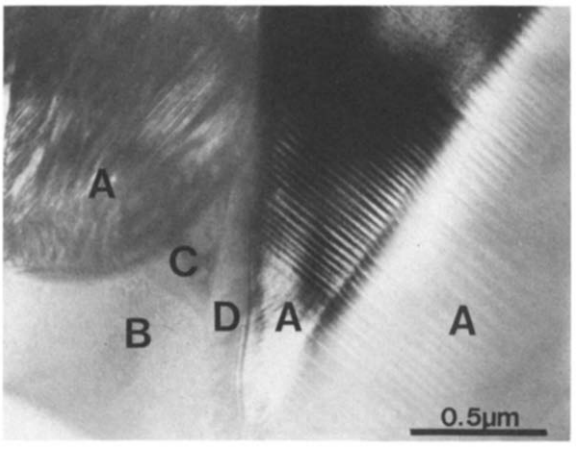

(a)

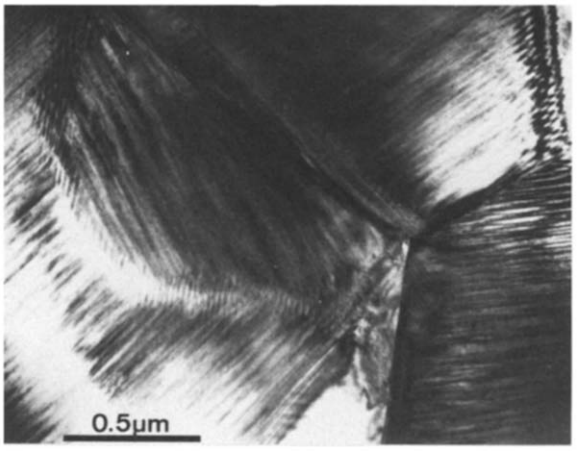

(b)

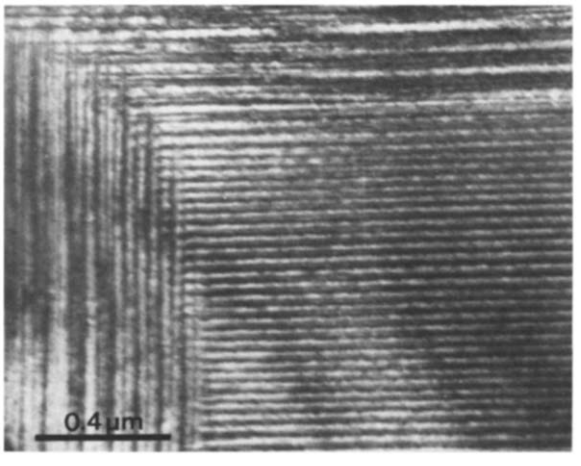

(c)

Fig. 2. Transmission electron micrographs (bright field) of $Mn_{2\cdot25}Ni_{0\cdot75}O_4$ (air quenched). (a) Spinel manganite grains: (A: Mn/Ni ≈ 4); NiO grains (B: Ni/Mn ≈ 9); (C: Ni/Mn ≈ 3); (D: Ni/Mn ≈ 8); (b) several sets of lamellae in different spinel manganite grains; (c) two sets of {110} lamellae in a spinel manganite grain. The electron beam is parallel to [001] and the lamellae are viewed edge-on.

3.1.2 Mn_2NiO_4

3.1.2.1 Slowly cooled. Two phases were detected by electron diffraction (Fig. 3): spinel manganite and nickel oxide, both free from lattice defects. EDX analysis shows that the cubic spinel manganite ($a = 0{\cdot}840 \pm 0{\cdot}001$ nm) is formed mainly of fairly homogeneous grains. The grain size (5–10 μm) is smaller than that of samples having a lower Ni content. The Mn content ranges from 72 to 76 at.% and the Ni content from 24 to 28 at.%. The Mn/Ni atomic ratio then becomes around 2·8 instead of 2, as calculated from the theoretical chemical formula. Moreover, very heterogeneous grains are observed, located

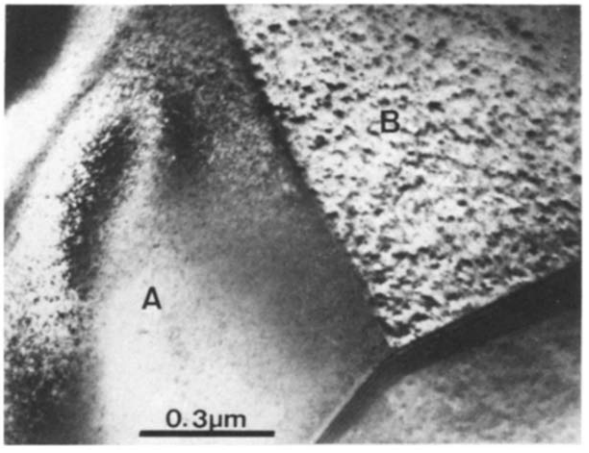

Fig. 3. Transmission electron micrograph (bright field) showing spinel manganite (A) and NiO (B) grains in Mn_2NiO_4 slowly cooled.

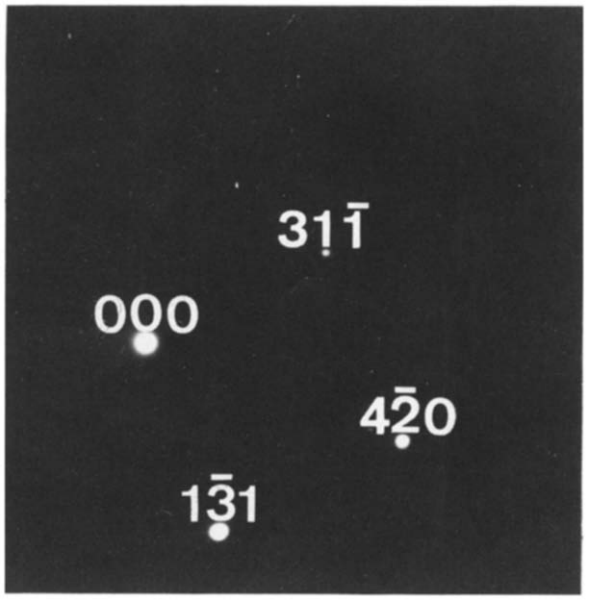

(a)

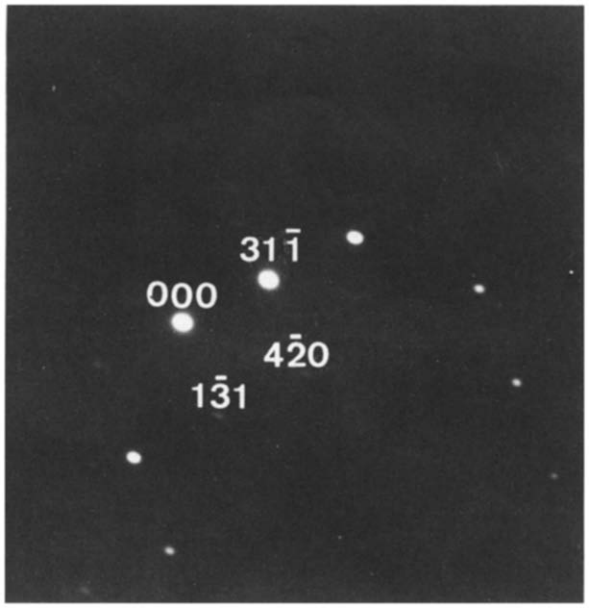

(b)

Fig. 4. Electron diffraction patterns of Mn_2NiO_4 slowly cooled. (a) Nickel oxide NiO with zone axis [1 2 5]; (b) nickel oxide with spinel manganite inclusions with zone axis [1 2 5].

immediately close to the NiO grains, with a Mn/Ni atomic ratio ranging from 0·4 to 3.1

The nickel oxide grains are smaller in size (1–2 μm). This phase has a NaCl cubic structure with $a = 0{\cdot}419 \pm 0{\cdot}003$ nm (measured from electron diffraction patterns) that is very close to the half value of the manganite cell. A simultaneous electron diffraction pattern of both phases in fact reveals that half of the reflexion spots coincide exactly, resulting from the perfect cube/cube orientation relationship between them (Fig. 4).

3.1.2.2 Air quenched. After quenching, both phases were still observed:

—Spinel manganite: cubic structure ($a = 0{\cdot}840 \pm 0{\cdot}001$ nm). Microanalysis of the metal elements in the spinel structure (Mn = 83 at.%, Ni = 17 at.%, Mn/Ni = 4·9) reveals that just over half of the Ni atoms are transformed into NiO. A characteristic TEM image of a manganite grain (Fig. 5) shows that a set of microtwin lamellae has developed parallel to the {111} planes. The orientation of these wedge-shaped microtwins indicates that they originate from the grain boundary that adjoins a NiO grain. Most of the manganite grains contain numerous microtwins, particularly when they adjoin a NiO grain, but only a single set of {111} twins is generally activated.

—Nickel oxide: as in the preceding case, the grains have a perfect orientation relationship cube/cube with manganite grains. Dark-field images (Fig. 6), using a manganite spot as operative reflexion, reveal that small inclusions of manganite are present in the NiO grain, having the same orientation relationship cube/cube. These inclusions have prismatic shapes with {110} facets and sizes range from 5

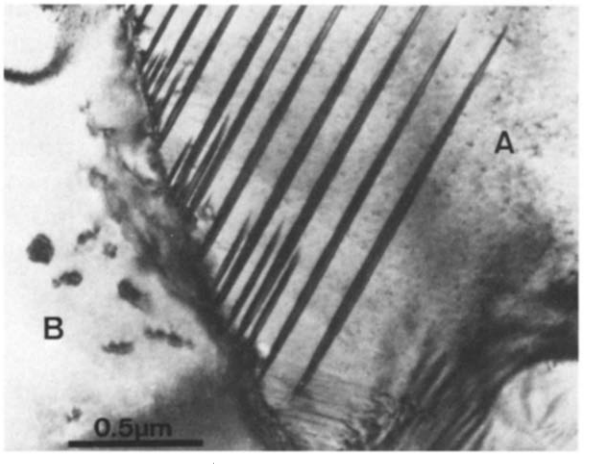

Fig. 5. Transmission electron micrograph (bright field) of Mn_2NiO_4 air quenched showing a boundary between a NiO grain (B) and a spinel manganite grain (A). Note the {111} microtwins originating from the interphase boundary.

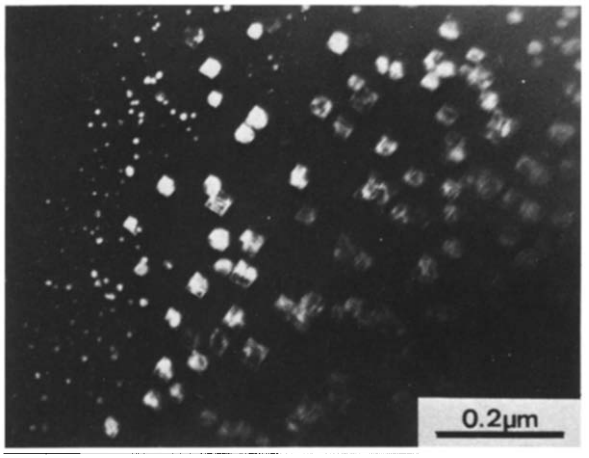

Fig. 6. Transmission electron micrograph (dark field with a manganite spot as operative reflection) showing prismatic spinel manganite inclusions in a NiO grain. Mn_2NiO_4 air quenched.

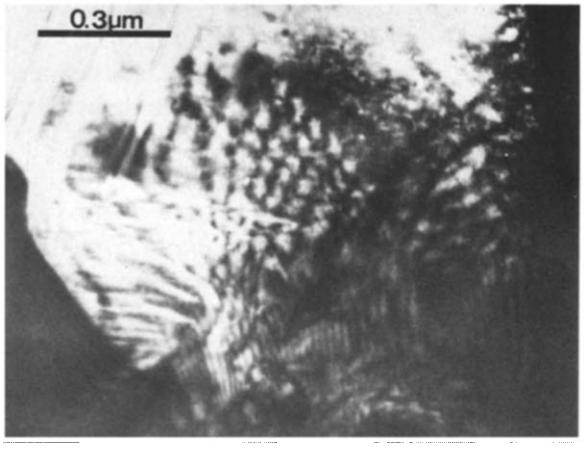

Fig. 7. Transmission electron micrograph (dark field with a manganite spot as operative reflection) showing spinel manganite (bright zones) and NiO (dark zones) closely mixed in a grain. Mn_2NiO_4 air quenched.

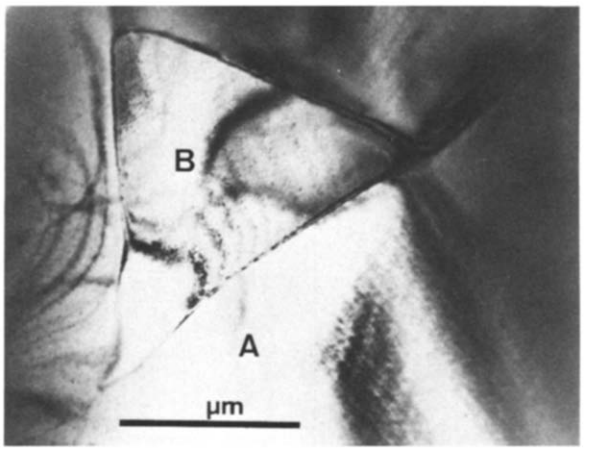

Fig. 8. Transmission electron micrograph (bright field) showing spinel manganite (A) and NiO (B) grains in $Mn_{1\cdot85}Ni_{0\cdot75}Co_{0\cdot4}O_4$ slowly cooled.

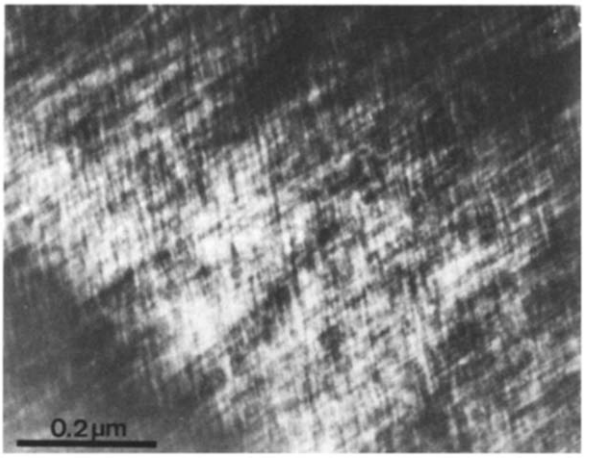

Fig. 9. Transmission electron micrograph (bright field) showing the 'tweed' structure in a manganite grain in $Mn_{1\cdot85}Ni_{0\cdot75}Co_{0\cdot4}O_4$ slowly cooled.

to 30 nm. This observation has been made for several NiO grains. Microanalysis of NiO grains (Ni = 79·5–83·6 at%, Mn = 16·4–20·5 at%) confirms the presence of small manganite inclusions in the NiO.

Moreover, some disturbed mixed zones, like that in the bottom of the studied area of Fig. 5, are observed: a dark-field image (Fig. 7) with a manganite spot shows that both phases are probably closely mixed there, forming lamellae of alternative NiO and manganite.

3.2 Nickel and cobalt manganite $Mn_{1\cdot85}Ni_{0\cdot75}Co_{0\cdot4}O_4$

3.2.1 Slowly cooled

The sample was biphased (Fig. 8): cubic spinel manganite ($a = 0\cdot834 \pm 0\cdot001$ nm) and nickel oxide. From X-ray diffraction, a slight tetragonalization of the cubic lattice of some manganite grains was deduced. The spinel phase (grain size 10–20 μm) is fairly homogeneous: Mn = 65·7–67·7 at.%, Co = 13·4–14·7 at.%, Ni = 18·9–20·1 at.%. Compared with the theoretical values (Mn = 61·7 at.%, Co = 13·3 at.%, Ni = 25 at.%), microanalysis shows that the sample is richer in Mn, and poorer in Ni than expected. The 'tweed' structure (Fig. 9) with lines parallel to {110} traces is observed.

In the NiO grains (size ≈ 1–$2\,\mu$m), prismatic manganite inclusions (size 20–30 nm) are observed always perfectly epitaxed. The atomic composition of these grains (Ni = 81·1–90·8 at.%, Co = 5·0–6·5 at.%, Mn = 3·4–12·7 at.%) shows that Co and Mn atoms are present in the lattice.

3.2.2 Air quenched

Two phases were also identified: spinel manganite and nickel oxide (Fig. 10(a)). The spinel phase is again tetragonalized, since the {311} {113} X-ray diffraction line is split but the tetragonalization is more important than in the slowly cooled samples. In the tetragonalized grains, planar defects parallel to {110} are numerous (Fig. 10(b)). The 'tweed' structure is also observed in some grains that seem to have the cubic structure ($a = 0\cdot836 \pm 0\cdot001$ nm).

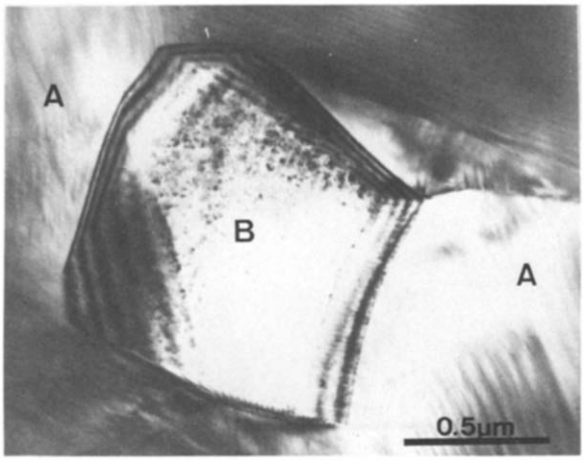

(a)

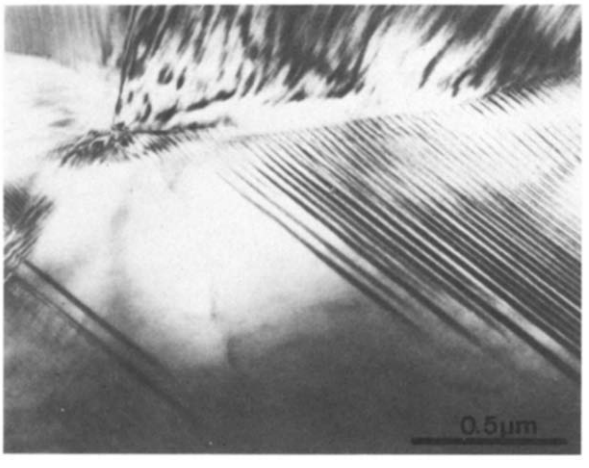

(b)

Fig. 10. Transmission electron micrograph (bright field) of $Mn_{1.85}Ni_{0.75}Co_{0.4}O_4$ air quenched: (a) NiO grain (B) surrounded by spinel grains (A); (b) planar defects parallel to {110} in manganite grains. The 'tweed' structure is visible on the bottom left corner of the picture.

The measured atomic composition (Mn = 68·9–71·3 at.%, Co = 11·2–13·4 at.%, Ni = 17·5–18·0 at.%) shows that the Ni atoms are in lower proportions than expected, as in the slowly cooled sample.

In the NiO grains (size $\approx 1\ \mu m$), Co and Mn atoms are present (Mn = 10–11 at.%, Co = 13–15 at.%, Ni = 75–76 at.%). Inclusions of small manganite grains are also likely but have not been imaged.

4 Discussion

The preparation of ceramics starts from monophased manganite powders; during the sintering at temperature higher than 1000°C, due to the instability of Mn^{4+} ions, phase separation occurs, yielding NiO out of the spinel lattice through Mn^{4+} reduction. These transformations are reversible so that a very slow cooling can yield again a single homogeneous phase. In contrast, a fast cooling freezes the biphased NiO–spinel manganite mixture. Note that when the sample is Ni-rich and even if it is slowly cooled, the NiO cannot entirely enter again the spinel structure by diffusion so that NiO is observed as intergranular precipitates.

The slowly cooled monophased $Mn_{2.25}Ni_{0.75}O_4$ ceramic has poor electrical stability $\Delta R/R$ (cf. Table 1), whereas after quenching stability is improved ($\Delta R/R = 2{\cdot}8\%$) and the NiO phase is observed. Nevertheless, the slowly cooled Mn_2NiO_4 ceramic is biphased (spinel and NiO), and $\Delta R/R$ is significant (about 9%). It is therefore suggested that the presence of the nickel oxide does not provide an improvement in the $\Delta R/R$ ratio. The authors do not consider that there is any correlation between the presence of the precipitated phases in the spinel matrix and the stability of the electrical properties.

As shown in Table 1, quenching improves the electrical stability of the compound. On the other hand, TEM observations reveal that, as is generally expected, quenching generates lattice defects in the manganite grain: mainly planar defects in the {111} or {110} planes.

The existence of the {111} microtwins in the quenched Mn_2NiO_4 ceramic is clearly related to the presence of nickel oxide. It has been noted that the twins generally originate from grain boundaries between spinel and nickel oxide. Since the misfit between both phases seems to be negligible, according to electron diffraction patterns, the stress accounting for the twin nucleation at the grain boundaries is mainly due to the difference in the thermal expansion coefficient of both phases. In addition it is noted that these grain boundaries do not generally coincide with low-index crystallographic planes, which are not planes of symmetry; thus only one set of microtwins is preferentially activated by thermally induced stresses.

The {110} planar defects which appear as extended lamellae (15–60 nm in width) were observed in the tetragonalized spinel grains. The 'tweed' structure (a few nm in width) was observed in two quenched samples ($Mn_{2.25}Ni_{0.75}O_4$ and $Mn_{1.85}Ni_{0.75}Co_{0.4}O_4$) but also in the slowly cooled $Mn_{1.85}Ni_{0.75}Co_{0.4}O_4$; the grains having this microstructure seem to have a cubic spinel structure, at least a tetragonalization is not detectable by electron diffraction.

The so-called 'tweed' structure, as well as the {110} extended lamellae, forms a modulated structure (exsolutions) that could result from the decomposition of the solid solution during the cooling. In the present case it is possible that these lamellae are alternatively Mn-rich and Ni-rich, or in the second case Ni-rich and Co-rich. They would result from diffuse segregation of Mn and Ni atoms, or Ni and Co atoms. Exsolutions are often observed in

alloys[8,9] and minerals,[10,11] and can originate via two distinct mechanisms: spinodal decomposition or nucleation (homogeneous or heterogeneous) and growth. Detailed experiments are required to determine the particular exsolution mechanism operating.

Another possibility is that the {110} lamellae originate from a cubic ----→ tetragonal transition resulting in transformation twins as it is observed in perovskite-based superconductors.[12]

It is noteworthy that the most satisfactory values of $\Delta R/R$ are generally obtained from samples presenting this 'tweed' structure. Recent TEM observations (forthcoming publication) on the Ni–Cu Ba-doped manganite confirm this result. Then it is suggested that the 'tweed' structure could be related to good electrical stability. On the other hand, the presence of {111} microtwins does not seem to be a guarantee of electrical stability.

It is well known that the semiconductor properties of NTC ceramics result from the existence of Mn^{3+}–Mn^{4+} pairs located in the octahedral sublattice of the spinel structure. The electrical conductivity of the compounds is strongly related to both on the pair concentrations and configurations.

Several authors[13–16] have shown that the Mn^{3+} ions located on the octahedral sublattice of the spinel structure gather in clusters and alter the electrical properties. The cluster dimensions decrease with increasing temperature and can be stabilized at room temperature according to the cooling rate of the samples.[13] Electrical instability would originate in the rearrangement of the Mn^{3+} ions at low temperature and the presence of defects could impede the mobility of Mn^{3+} ions and then improve the electrical stability.

5 Conclusion

The TEM observations give additional information on the part played by the precipitates and the lattice defect in the electrical stability of ceramics. It has been shown in particular that:

(i) The precipitated phase (NiO) on the grain boundaries does not seem to influence electrical stability;
(ii) the bi-dimensional modulated structure ('tweed' structure) could be accounted for by the improvement in electrical stability, the migration of clusters then being disturbed by these exsolution defects.

Acknowledgements

The authors thank J. Sarrias of L.C.M.I. URA 1311, who prepared the ceramics from highly pure powders and who performed the sintering, and L. Bernard of I.N.S.A. URA 74, for difficult and careful sample preparation for TEM.

References

1. Vervey, E. J. M., Haaij, P. W., Romeijn, F. C. & Van Oosternout, C. W., Controlled-valency semiconductors. *Philips Res. Rep.*, **5** (1950) 173–87.
2. Macklen, E. D., *Thermistors*. Electrochemical publications Ltd, Ayr, Scotland, 1979.
3. Caffin, J. P., Elaboration et caractérisation de céramiques semi-conductrices à base de manganites de cuivre et de nickel. Stabilisation des propriétés électriques des thermistances à coefficient de température négatif (C.T.N.) à faibles résistivités. PhD thesis, Institut National Polytechnique, Toulouse, France, 1986.
4. Caffin, J. P., Rousset, A., Carnet, R. & Lagrange, A., Chemical preparation of N.T.C. thermistors with low resistivity and high stability. In *Proceeding of the High Tech. Ceramics*, ed. P. Vincenzini. Elsevier Science Publishers B.V., Amsterdam, 1987, pp. 1743–51.
5. Rousset, A., Legros, R., Caffin, J. P. & Lagrange, A., Stabilisation des propriétés électriques des thermistances C.T.N. à faibles résistivités. In *Proceedings of the 2nd Colloque International sur les Composants Passifs*, ed. Ministry of Research and Technology, Paris, 1987, pp. 382–5.
6. Metz, R., Legros, R., Rousset, A., Caffin, J. P., Loubière, A. & Bui, Ai, The N.T.C. thermistors of low resistivity and large stability. *Silicates Industriels*, **34** (1990) 71–6.
7. Legros, R., Metz, R., Caffin, J. P., Lagrange, A. & Rousset, A., Controlled morphology in electronic ceramic powder preparation. In *Proceedings of the Better Ceramics through Chemistry III*, ed. C. J. Brinker *et al.* Elsevier Science Publishers, NY, **121**, 1988, pp. 251–6.
8. Shultz, A. H. & Stubican, V. S., Modulated structures in the system TiO_2–SnO_2. *Phil. Mag.*, **18** (1968) 929–37.
9. Ardell, A. J., Nicholson, R. B. & Eshelby, J. D., On the modulated structure of aged Ni Al alloys. *Acta Met.*, **14** (1966) 1295–309.
10. Carstens, H., Exsolutions in ternary feldspars. I: On the formation of antiperthites. *Contrib. Mineral Petrol.*, **14** (1967) 27–35.
11. Willaime, C. & Gandais, M., Study of exsolutions in alkali feldspars. Calculation of elastic stresses inducing periodic twins. *Phys. Stat. Sol.(a)*, **9** (1972) 529–39.
12. Zhu, Y., Tafto, J. & Suenaga, M., Defects in high T_c cuprate superconductors. *M.R.S. Bulletin*, **11** (1991) 54–8.
13. Kripicka, S., Simsa, Z. & Smetana, Z., The influence of Mn^{3+} clusters on the physical properties of Mn-Fe spinels. *Czech. J. Phys.*, **B18** (1968) 1016–25.
14. Brabers, V. A. M., Cation migration, cation valencies and the cubic–tetragonal transition in $Mn_xFe_{3-x}O_4$. *J. Phys. Chem. Solids*, **32** (1971) 2181.
15. Vandenberghe, R. E., Brabers, V. A. M. & Robbrecht, G. G., The preparation and the lattice parameters of cubic $CuMn_{3-x}O_4$ spinels. *Phys. Stat. Sol.(a)*, **16K** (1973) 117–20.
16. Jarrige, J., Etude des manganites de cuivre. PhD Thesis No. 79-5, University Limoges, France, 1979.